Plant Growth Regul (2017) 82:479–489
DOI 10.1007/s10725-017-0274-3

ORIGINAL PAPER

Isolation and functional analysis of *MxCS3*: a gene encoding a citrate synthase in *Malus xiaojinensis*, with functions in tolerance to iron stress and abnormal flower in transgenic *Arabidopsis thaliana*

Deguo Han[1] · Yufang Wang[1] · Zhaoyuan Zhang[1] · Qianqian Pu[1] · Haibin Ding[1] · Jiaxin Han[1] · Tingting Fan[1] · Xue Bai[1] · Guohui Yang[1]

Received: 1 August 2016 / Accepted: 17 April 2017 / Published online: 21 April 2017

Abstract Iron (Fe) is one of the essential micronutrients required by all plants. Citric acid is considered as the chelate substance in the long distance transport of Fe. In this study, a gene encoding putative citrate synthase was isolated from *Malus xiaojinensis* and designated as *MxCS3*. The *MxCS3* gene encoded a protein of 235 amino acid residues with a theoretical isoelectric point of 9.47 and a predicted molecular mass of 26.3 kDa. Subcellular localization study revealed that *MxCS3* is preferentially localized in mitochondrion and cytoplasmic membrane. The expression of *MxCS3* was enriched in leaf, phloem, and root, which was highly affected by Fe stress, indoleacetic acid and abscisic acid treatment in *M. xiaojinensis* seedlings. When *MxCS3* was transferred into *Arabidopsis thaliana*, it improved Fe stress tolerance in transgenic *Arabidopsis*. Increased expression of *MxCS3* in transgenic *A. thaliana* also led to increased fresh weight, root length, CS activity, and the contents of chlorophyll, citrate acid, Fe and Zn, especially when dealt with Fe stress. More importantly, we firstly found that ectopic expression of *MxCS3* resulted in abnormal flowers in transgenic *Arabidopsis*.

Keywords Iron · *Malus xiaojinensis* · *MxCS3* · Transgenic *Arabidopsis* · Iron stress · Abnormal flower

✉ Deguo Han
deguohan_neau@126.com

✉ Guohui Yang
yangguohui_neau@126.com

[1] Key Laboratory of Biology and Genetic Improvement of Horticultural Crops of Northeast Region (Ministry of Agriculture), College of Horticulture & Landscape Architecture, Northeast Agricultural University, Harbin 150030, People's Republic of China

Introduction

Metal ions, such as Fe, Mn, Cu, and Zn are essential elements for plant growth and development (Marschner and Romheld 1994; Marschner 2012). Fe, however, has poor solubility in most soil types (Guerinot and Yi 1994), particularly in partial alkaline soil where the content of free Fe is far below 10^{-6} M, a required concentration for compatible plant growth (Han et al. 1998; Hell and Stephan 2003). Therefore, Fe deficiency is a worldwide problem for crop growth, development and production (Abadía et al. 2002). Fe deficiency-induced plant chlorosis in young leaves is a major global problem (Romheld and Marschner 1986; Ling et al. 1999), which is a common disease in apple, especially in North China, and largely limits the growth, yield and quality of apple (Yang et al. 2015).

To avoid such deficiencies, plants have developed adaptable mechanisms to acquire Fe from soil, which have been classified into two strategies (Strategy I and Strategy II) by Marschner and Romheld (1994). In response to Fe deficiency, all non-graminaceous plants appear to adopt 'Strategy I', the activity of citrate synthase (CS) and CA content increase (Han et al. 2015a). Regarding Fe deficiency-induced the citrate and other carboxylates increases have been reported in many species (Abadía et al. 2002), such as in fruit trees including kiwifruit (Rombolà et al. 2002), pear (López-Millán et al. 2001), Citrus (Martínez-Cuenca et al. 2013), etc. Fe-deficiency caused increase of CS activity, which has also been found in tomato (López-Millán et al. 2009) and pea (Jelali et al. 2010). Fe-deficiency also induced the increased expression of the *CS* gene in *Arabidopsis* (Thimm et al. 2001) and apple (Han et al. 2012, 2015b). Recently, this fact has also been reported in a study on barley (a Strategy II plant), which focused on the Fe deficiency-induced changes in

carboxylate metabolism in two cultivars of barley with different Fe efficiency responses (López-Millán et al. 2012). Additionally, CA can chelate Fe(III) for its long distance transportation through xylem (Cataldo et al. 1988; Rellán-Álvarez et al. 2010) in plants where the pH is about 5.5–6 (Hell and Stephan 2003). 'Strategy I' plants produce more ferric reductase–oxidase under Fe-deficiency stress, to reduce Fe(III) to Fe(II) and benefit Fe uptake (Zhang et al. 2009). The *Arabidopsis* mutant, *frd3*, has provided molecular evidence of the role of CA in long-distance Fe transport (Durrett et al. 2007).

The absorption and utilization of Fe in apple (*M. xiaojinensis* included) follows 'Strategy I' mechanism. Previous studies indicated that *M. xiaojinensis* is a Fe-efficient apple genotype (Han et al. 1998). A relevant number of molecular components involved in the high tolerance to Fe deficiency of *M. xiaojinensis* have been isolated and studied during the last decade. The expression of these genes was affected by Fe stress in *M. xiaojinensis* and transgenic plants had higher Fe stress tolerance than wild-type, which involved in the 'Strategy I' responses at different levels such as Fe acquisition and transport, and regulation of Fe responses. Most of these studies reported on the physiological and molecular components involved in acquisition and transport of Fe in *M. xiaojinensis*, such as *MxIRT1* by Li et al. (2006), *MxMYB1* by Shen et al. (2008), *MxSAMS* by Zhu et al. (2009), *MxNas1* by Zhang et al. (2009) and Han et al. (2013b), *MxbHLH01* by Xu et al. (2011), *MxVHA-c* by Zhang et al. (2012), *MxIRO2* by Yin et al. (2013). The *MxCS1* and *MxCS2* were also studied by Han et al. (2013a, 2015a), these results showed that the expression levels of *MxCS1* and *MxCS2* were affected by Fe stress and plant hormones (IAA and ABA) treatments. Over-expression of *MxCS1* and *MxCS2* improved Fe stress tolerance in transgenic *Arabidopsis* and tobacco. Increased expression of *MxCS1* in transgenic tobacco plants also resulted in early-flowering, morphological abnormalities flowers and increased concentrations of Fe, Mn, Cu, and Zn in young leaf and flower (Han et al. 2013a).

Moreover, some plant hormones such as IAA and ABA are considered as signals of Fe stress in *Arabidopsis* and tomato (Schikora and Schmidt 2001; Schmidt et al. 2000). The expression of *MxCS1* and *MxCS2* in *M. xiaojinensis* seedlings was affected by IAA and ABA treatments, and the expression levels increased in all parts of *M. xiaojinensis* (Han et al. 2013a, 2015a). Fe-deficiency also induced the increasing of IAA content in the shoot apex of *M. xiaojinensis* and treatments of IAA to the shoot apex triggered Fe deficiency responses (Wu et al. 2012).

In the present study, we isolated a new citrate synthase gene from *M. xiaojinensis*, designated it as *MxCS3*. The *MxCS3* is a new member of *M. xiaojinensis* citrate synthase gene family. The functions of *MxCS1* and *MxCS2* have been studied, which played a key role in synthesizing citrate synthase. In addition, the over-expression of *MxCS1* and *MxCS2* improved Fe stress tolerance in transgenic plants. However, whether another member of this gene family (*MxCS3*) has the similar function and which gene is the key gene of this family are still unknown. Furthermore, the relationship between *MxCS3* gene and Fe transport or plant development remains unclear. Through the experiment, we detected the expression level of *MxCS3* in different organs, and found the relationships between the expression of *MxCS3* and Fe stress, IAA and ABA treatments. Moreover, we found that ectopic expression of the *MxCS3* improved tolerance to Fe stress in transgenic *Arabidopsis thaliana*, but also led to increased fresh weight, root length, CS activity, and contents of chlorophyll, citrate acid and Fe, especially when dealt with Fe stress. More importantly, we first discovered that ectopic expression of *MxCS3* resulted in abnormal flowers in transgenic *A. thaliana*.

Materials and methods

Plant material and growth conditions

Malus xiaojinensis test-tube seedlings were rapidly propagated on Murashige and Skoog medium (MS) + 0.5 mg L^{-1} IBA + 0.3 mg L^{-1} 6-BA for 40 days, and then returned to MS +1.2 mg L^{-1} IBA for 45 days for rooting. Finally, the seedlings were transferred to Hoagland solution for 50 days for growth. When the plants had 8–9 mature leaves (fully expanded), they were exposed to Hoagland nutrient solutions with different Fe concentrations (4, 40, and 160 μM). For IAA and ABA treatments, seedlings were respectively put into 0.1 mM IAA and 0.1 mM ABA Hoagland solution with normal Fe concentration (Han et al. 2013b). The root, phloem, xylem and leaf samples of all control and treated plants were sealed after treatments of respectively 0, 2, 4, 8, and 12 h, immediately frozen in liquid nitrogen, and then stored at −80 °C for RNA extraction.

Isolation and real-time PCR expression analysis of *MxCS3*

Total RNA was respectively extracted from root, phloem, xylem, new leaf (partly expanded), and mature leaf using the CTAB method (Han et al. 2015a). First strand cDNA was synthesized with 1 μg total RNA and 1 μL super script II enzyme (Invitrogen, USA) according to the manufacturer's protocol. PCR was performed to obtain a whole sequence of *MxCS3* by using the first strand cDNA of *M. xiaojinensis* as a template. A pair of primers (F1, 5′-ATGGTATTCTTCACGAGCGTCAC-3′ and F2, 5′-CTATGAGAGAGATGTAATATGCTTTACC-3′)

was designed based on the homologous regions of *MdCS3* (MDP0000913825) to amplify the full-length cDNA sequence. The full-length cDNA of *MxCS3* gene was isolated from *M. xiaojinensis* using nested PCR with F1 and F2 as primers twice. The obtained DNA fragments were gel purified and cloned into the pMD18-T vector (Takara) and sequenced (Invitrogen, Beijing).

Real-Time PCR expression analysis of *MxCS3* methods was performed according to Jiang and Zhou (2016). As a control, the *18S rRNA* gene was amplified from *M. xiaojinensis* tissues using the following primers: *Mx18SF*, 5′-ACACGGGGAGGTAGTGACAA-3′ and *Mx18SR*, 5′-CCTCCAATGGATCCTCGTTA-3′, which were designed from the sequences published in the GenBank databases. For real-time PCR detection, the primers of *MxCS3* were designed from partial sequences isolated in this study, which are MF, 5′-GAACGTCTGAAGAAACTGAAGGCA-3′ and MR, 5′-GCTGGAACTACAGCACGAGTCCT-3′, respectively. The thermal cycling program was one initial cycle of 93 °C for 30 s, followed by 40 cycles of 93 °C for 5 s, and 58 °C for 30 s. The relative transcription level data was analyzed using the $2^{-\Delta\Delta CT}$ method (Livak and Schmittgen 2001).

Subcellular localization of the MxCS3 protein

The *MxCS3* ORF was cloned into the *Sac*I and *Kpn*I sites of the pSAT6-GFP-N1 vector. This vector contains a modified red shifted green fluorescent protein (GFP) at *Sac*I–*Kpn*I sites. The *MxCS3*–GFP construct was transformed into onion (*Allium cepa*) epidermal cells by particle bombardment as described earlier (Yang et al. 2015). The Clone MTC754 (ScyTek, USA) was used as mitochondrial marker for mitochondrion detection. The transient expression of the *MxCS3*–GFP fusion protein was observed under confocal microscopy.

Arabidopsis thaliana transformation

To construct an expression vector for transformation of *A. thaliana*, restriction enzyme cut sites of *Sma*I and *Eco*RI were added into *MxCS3* cDNA at both 5′ and 3′ ends by PCR. To construct the pBI121-*MxCS3* vector, the products of PCR and pBI121 were digested by *Sma*I and *Eco*RI, and linked together through the replacing of *GUS* gene. The *MxCS3* gene driven under CaMV 35S promoter was introduced into *Arabidopsis* plants by *Agrobacterium*-mediated GV3101 transformation (An et al. 1988). Columbia ecotype *A. thaliana* plants were transformed using the vacuum infiltration method. Transformants were selected on MS medium containing 50 mg dm^{-3} Kanamycin. T_3 generation plants were used for further analysis.

Germination and growth assay

The T_3 generation transgenic *A. thaliana* were used in the subsequent experiments. For the growth assay, T_3 transgenic plants lines and wild-type seeds were placed on MS agar plates for germination. After 6 days, 30 germinated seedlings from each line were carefully transferred to new MS agar plates supplemented with 4 (low concentration), 100 (normal level), 400 μM (high concentration) Fe, respectively. After 14 days growth in treatment medium, the development conditions were observed and the root length (total length of each plant) and fresh weight of seedlings were measured. Twenty strains transgenic *A. thaliana* for each experimental line (OE-4 and OE-5) were collected together and used in the present experiments. Each index was measured for five times, three replicates were conducted and the standard deviation (±SD) were measured.

Detection of the contents of chlorophyll, Fe, Zn and CA and CS activity

Chlorophyll contents were measured according to the method of Aono et al. (1993). According to Takahashi et al. (2003), Fe and Zn concentrations in leaf were measured. Assays for the content of citric acid were performed by HPLC method (López-Millán et al. 2009) with a Waters HPLC system, including a 600E pump, a 996 photodiode array detector and the Millenium 2010 software. Samples were injected with a Rheodyne injector (20 μL loop). Mobile phase was pumped at a 0.7 mL min^{-1} flow rate. Quantification was carried out with pure citric acid (Sigma, USA) as an external standard. According to Leek et al. (2001), the CS activities of all kinds of *A. thaliana* (*MxCS3*-OE and WT lines) in leaf were measured.

Observation and record of the flowers of *Arabidopsis thaliana*

The transgenic *Arabidopsis* for each experimental line (OE-4 and OE-5) T_3 transgenic plants and wild-type seeds were placed on MS agar plates for germination. Then, 50 germinated seedlings from each line were carefully transferred to culture matrix (nutrient soil:vermiculite ratio is 4:1) with normal water management in a light growth chamber at 25 ± 1 °C under a 16 h light (120 μmol m^{-2} s^{-1}) / 20 ± 1 °C under a 8 h dark regime. When most of *Arabidopsis* were in full bloom, 100 flowers of each line were collected, observed and recorded with stereomicroscope (Olympus BX51). As a reference factor, the number of petals of each line (OE-4, OE-5 and WT) was also statistically analyzed (100 flowers were collected from each *A. thaliana* line at 8:00 AM). Three replicates were conducted and the standard errors (±SE) were calculated.

Results

Isolation of *MxCS3* gene from *M. xiaojinensis*

Sequence analysis showed that the *MxCS3* cDNA is a complete open reading frame of 708 bp, and the predicted MxCS3 protein comprises 235 amino acids with a theoretical isoelectric point of 9.47 as well as a predicted molecular weight of 26.3 kDa. The *MxCS3* gene sequence and amino acid sequence of the MxCS3 protein are presented with citrate synthase domain underlined in Fig. 1.

Phylogenetic relationship of MxCS3 with other CS proteins

To investigate the evolutionary relationship among plant CS proteins, eight CS proteins from different species were analyzed by DNAman analyse software (Fig. 2). As shown in Fig. 2a, the deduced amino acid sequence of MxCS3 includes one conserved CS domain in the C-terminal region. The citrate synthase domain contains the plant-specific GKVQLGNITV sequence which serves as a DNA-binding motif of CS (Alexandrov et al. 2006; Han et al. 2013a).

Comparing the amino acid sequences of MxCS3 with other CS proteins, we found that MxCS3 has a high identity to the CS protein family. Additionally, a phylogenetic tree (neighbour-joining) was constructed with the full-length amino acid residues (Fig. 2b) by DNAman. The results showed that MxCS3, MdCS3 (*M. domestica*), MxCS1 (*M. xiaojinensis*, Han et al. 2012) and PpCS3, *CS* protein from peach (Etienne et al. 2002) clustered together. AtCS4, *CS* protein from *A. thaliana* (Alexandrov et al. 2006), DcCS3, *CS* protein from carrot (Takita et al. 1999) and NtCS, *CS* protein from tobacco were grouped into another cluster. However, OsCS, *CS* protein from rice was the third cluster alone.

Subcellular localization of MxCS3

The presence of a CS synthase, which has a citrate synthase domain, suggests that *MxCS3* is a functional gene. As shown in Fig. 3, the MxCS3–GFP fusion protein is targeted into mitochondrion and cytoplasmic membrane, whereas the control GFP alone is distributed throughout the cytoplasm. These results showed that MxCS3 is a mitochondrion and cytoplasmic membrane localization protein.

Expression analysis of *MxCS3* in *M. xiaojinensis*

The expression profile of the *MxCS3* in various *M. xiaojinensis* tissues under normal Fe treatment (40 μM) was investigated by using real-time PCR assay. Expression of *MxCS3* was enriched in leaf, root and phloem of stem, but very low in the xylem (Fig. 4a). The results showed that *MxCS3* mRNA increased in new leaf, phloem and root, under a low Fe concentration (4 μM), IAA, and ABA conditions (Fig. 4b, d, e) at the beginning and reached the maximums at 8 h, then decreased slightly at 12 h, whereas the expression level of *MxCS3* in these parts decreased under a high Fe (160 μM) stress. The expression level of *MxCS3* in mature leaf was just opposite to the above parts under Fe stress concentration and had the same trend when dealt with IAA and ABA (Fig. 4c).

Ectopic expression of *MxCS3* confers tolerance to Fe stress in transgenic *A. thaliana*

In order to investigate the role of *MxCS3* in response to Fe stress in plants, we generated transgenic *A. thaliana* with ectopic expression of *MxCS3* under the control of the

```
1   ATGGTATTCTTCACGAGCGTCACCGCGCTATCCAAGCTCCGTTCTCGTCTCGGGCAACGGTCGAGTCTCAGGGATTCCGTCAGATGGATTCAAACGCAGACC
1    M  V  F  F  T  S  V  T  A  L  S  K  L  R  S  R  L  G  Q  R  S  S  L  R  D  S  V  R  W  I  Q  T  Q  T

103 TCCACAGATCTCGACCTTCGTTCTCAGTTGGCGGAATTGATTCCAGAACAACAGGAACGTCTGAAGAAACTGAAGGCAGATTATGGAAAAGTTCAACTGGGC
35   S  T  D  L  D  L  R  S  Q  L  A  E  L  I  P  E  Q  Q  E  R  L  K  K  L  K  A  D  Y  G  K  V  Q  L  G

205 AATATCACGGTTGATATGGTGATTGGTGGAATGAGAGGAATGACAGGGTTGCTGTGGCAAACCTCCTTACTTGATCCAGATGAGGGAATTCGCTTCAGGGGT
69   N  I  T  V  D  M  V  I  G  G  M  R  G  M  T  G  L  L  W  Q  T  S  L  L  D  P  D  E  G  I  R  F  R  G

307 GTGTCAATTCCAGAATGCCAGAAAGTATTACCTGCTGCAAAGCCAGGTGGAGAACCTCTGCCTGAGGGTCTTCTGTGGCTGCTTGTGACAGGAAAGGTACCT
103  V  S  I  P  E  C  Q  K  V  L  P  A  A  K  P  G  G  E  P  L  P  E  G  L  L  W  L  L  V  T  G  K  V  P

409 AGCAAAGAGCAAGTAGATGCATTATCCAAGGAATTGAGGACTCGTGCTGTAGTTCCAGCTTATGTGTATAAGGCCATTGATGCTCTGCCTATAACAGCACAT
137  S  K  E  Q  V  D  A  L  S  K  E  L  R  T  R  A  V  V  P  A  Y  V  Y  K  A  I  D  A  L  P  I  T  A  H

511 CCAATGACCCAGTTCACCACTGGTGTCATGGCGCTCCAGGTAGACAGTGAATTCCAGAAGGCATATGAAAAGCGGATACATAAATCAAAGTACTGGGAGCCA
171  P  M  T  Q  F  T  T  G  V  M  A  L  Q  V  D  S  E  F  Q  K  A  Y  E  K  R  I  H  K  S  K  Y  W  E  P

613 ACTATTGAGGATTCACTTAGCTTGATTGCACAAGTGCCAGTAGTAGCTGCCTATATTTATCGAAGGTTGGTAAAGCATATTACATCTCTCTCATAG
205  T  I  E  D  S  L  S  L  I  A  Q  V  P  V  V  A  A  Y  I  Y  R  R  L  V  K  H  I  T  S  L  S  *
```

Fig. 1 Nucleotide and deduced amino acid sequences of *MxCS3*. The citrate synthase domain is *underlined*

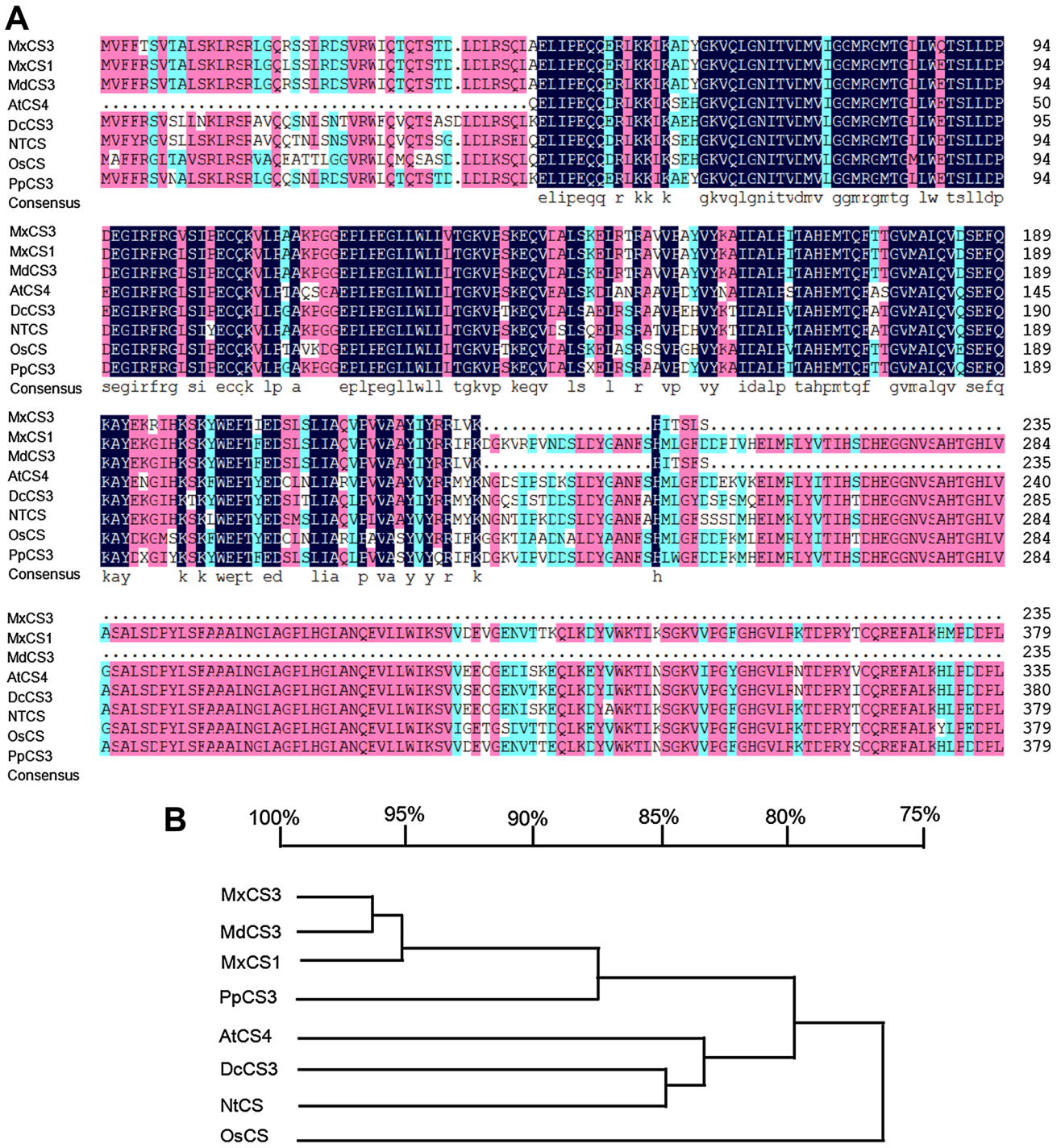

Fig. 2 Comparison and phylogenetic relationship of MxCS3 with other reported citrate synthase proteins. **a** Positions containing identical residues are shaded in *navy blue*, while conservative residues are shown in *green* (*top*). **b** Phylogenetic tree analysis of MxCS3 and other plant citrate synthase proteins. The tree was constructed by the neighbour-joining method with DNAman. The gene accession numbers are listed as follows:[*MdCS3* (XM_008376898.2), *MxCS1* (ADL62695.1), *PpCS3* (AAL11504.1), *AtCS4* (AAM62868.1), *DcCS3* (AB017159.1), *NtCS* (CAA59008.1) *OsCS* (AAG28777.1)]. (Color figure online)

CaMV 35S promoter. Among ten transformed lines, six of them (OE-1, OE-3, OE-4, OE-5, OE-7 and OE-9) were confirmed by using RT-PCR analysis with WT line (wild-type) as control (Fig. 5a).

No significant difference in appearance between WT line and *MxCS3*-OE *A. thaliana* lines was observed. The T_3 transgenic lines OE-4, OE-5 and WT seedlings were placed on MS agar plates supplemented with 4 (low Fe stress), 100

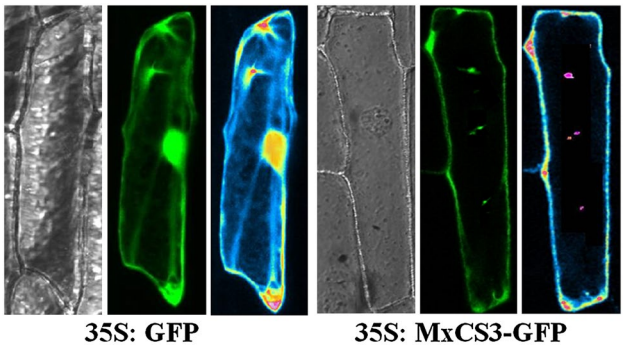

Fig. 3 Subcellular localization of MxCS3. Transient expressions in onion epidermal cells of 35S-GFP and 35S-MxCS3-GFP translational product were visualized by fluorescence microscopy. The transient vector harboring 35S-GFP and 35S-MxCS3-GFP cassettes were transformed into onion epidermal cells by particle bombardment. The photos were taken in the *bright light* (*left*), in the *dark* for GFP images (*middle*), the mitochondrial detection (*red colour*) in the *dark* (*right*) after incubation for 26 h. (Color figure online)

(normal Fe level), 400 μM (high Fe stress) Fe. As shown in Fig. 5b, after 14 days growth in treatment medium, the appearances were observed. On normal Fe level agar plates, all types of *Arabidopsis* grew well. WT line had obvious chlorosis appearance, but *MxCS3*-OE lines (OE-4 and OE-5) had no obvious chlorosis appearance on Fe-deficiency (4 μM) agar plates. *MxCS3*-OE lines also had better appearance than WT line on high Fe concentration (400 μM) agar plates.

The *MxCS3*-OE lines (OE-4 and OE-5) had higher fresh weight and longer root length than WT line (Table 1), especially when exposed to Fe stress. The fresh weight and root length of *MxCS3*-OE lines were respectively 2.5–2.8 folds and 1.7–2.3 folds higher than that of WT line. To determine the effect of Fe stress on different plants, the chlorophyll contents were measured in leaf from *MxCS3*-OE (OE-4 and OE-5) and WT lines. As shown in Table 1, the *MxCS3*-OE seedlings showed higher chlorophyll contents than that in WT line, especially when exposed to low or high Fe concentrations. The WT line was more wilted and yellow than those of transgenic *A. thaliana*, corresponding to lower chlorophyll contents.

As shown in Table 1, the *MxCS3*-OE lines showed higher CS activity than WT line, especially when grown on medium with low or high Fe concentration. The CS activities in *MxCS3*-OE lines under low and high concentrations were 5.2 and 4.2 folds higher than WT line, respectively. Fe and Zn contents of *MxCS3*-OE transgenic lines were higher than that of WT line in all kinds of MS media (different Fe concentrations). The content of citric acid was also measured in *A. thaliana* lines. As shown in Table 1, the transgenic seedlings showed higher contents of CA on all kinds of agar plates, especially when grown on media with low or high Fe stresses. The contents of CA in *MxCS3*-OE transgenic lines under low

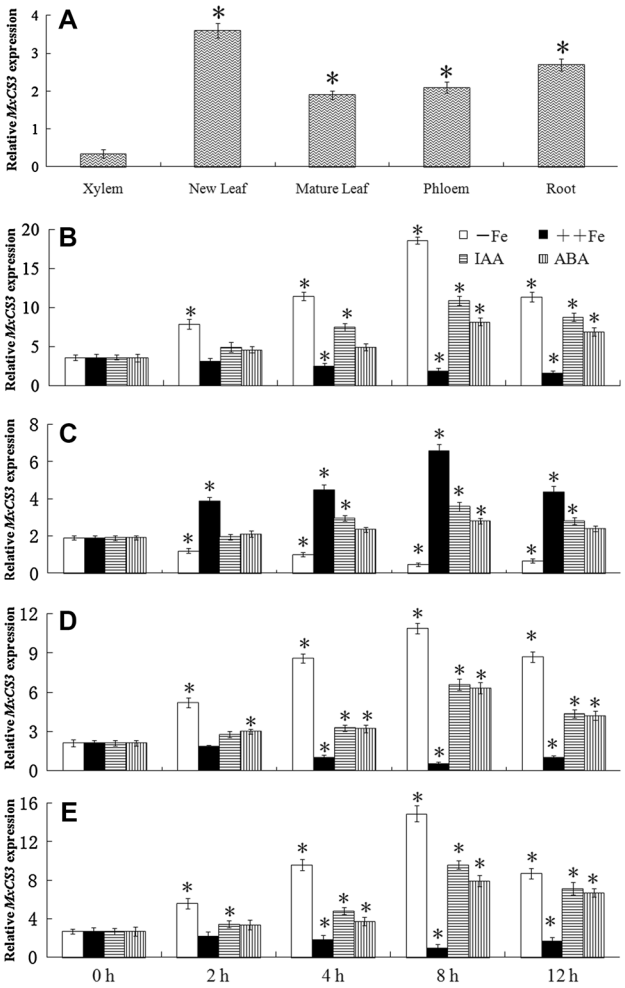

Fig. 4 Time-course expression patterns of *MxCS3* in *M. xiaojinensis* using real-time PCR. **a** Expression patterns of *MxCS3* in xylem, new leaf, mature leaf, phloem and root in normal Fe concentration (40 μM). **b–e** Expression patterns of *MxCS3* in a low concentration of Fe (4 μM,−*Fe*), high concentration of Fe (160 μM, ++*Fe*), dealt with 0.1 mM IAA (*IAA*) and 0.1 mM ABA (*ABA*) in new leaf (**b**), mature leaf (**c**), phloem (**d**) and root (**e**) at the following time points: 0, 2, 4, 8 and 12 h. The expression amounts were normalized to that of *Mx18S*. Each data (mean ± SD, n = 3) represents the average of three independent plants; *error bars* indicate the standard deviation. *Asterisks* above the *error bars* indicate a significant difference between the treatment and control (0 h) using Student's t test ($P \leq 0.05$)

and high concentrations were 3.3 and 3.8 folds, respectively, higher than that in WT line. Increased expression of *MxCS3* in transgenic *A. thaliana* also led to increased fresh weight, root length, and the contents of chlorophyll especially when dealt with Fe stress.

Ectopic expression of *MxCS3* resulted in abnormal flowers in transgenic *A. thaliana*

In addition to the changes of contents of chlorophyll and CA, the transgenic *MxCS3 A. thaliana* (OE-4 and OE-5)

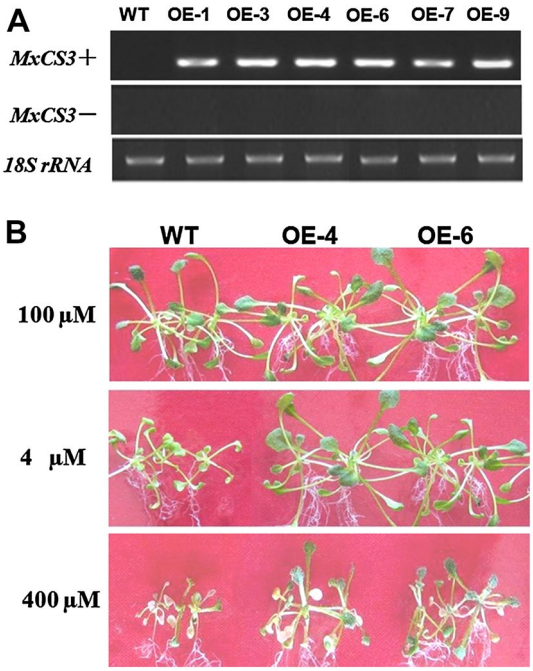

Fig. 5 Expression of *MxCS3* in transgenic *A. thaliana* and over-expression (OE) of *MxCS3* in *A. thaliana* improved Fe tolerance. **a** The expression level of *MxCS3* in wild type (WT) and *MxCS3*-OE transgenic T_1 lines. Ethidium bromide staining of PCR products using *MxCS3*-specicific primers with (*top*) and without (*middle*) prior reverse transcription, and the RT-PCR products with *18s rRNA* gene (*Mx18SF* and *Mx18SR*) primers (*bottom*); **b** Over-expression of *MxCS3* in *A. thaliana* improved Fe tolerance. The seedlings phenotype of WT and T_3 *MxCS3*-OE lines (OE-4 and OE-5) were germinated and grown on MS media supplied with 4, 100, 400 μM Fe for 14 days. All treatments are repeated at least three times and represented results were showed here

flowers developed markedly morphological abnormalities (Fig. 6). The flowers of WT *A. thaliana* had four calyxes, four petals, six stamens and only one pistil (Fig. 6a, f). In contrast, *MxCS3*-OE *Arabidopsis* produced two types of abnormally shaped flowers: (1) Abnormal shape of flower organs: curving and short calyx (Fig. 6h, i), curving petal (Fig. 6i) and short stamens (Fig. 6g, i); (2) Abnormal number of flower organs. This type of flower showed supernumerary calyxes, petals, stamens and pistils (Fig. 6b, d, g, i), or a decreased number of calyxes, petals and stamens (Fig. 6e, j) or supernumerary calyxes, petals and a decreased number of stamens (Fig. 6c, h).

As one of the reference factors, the number of petals of transgenic *MxCS3 A. thaliana* (OE-4 and OE-5) changed markedly (Fig. 7). The results showed that the largest proportion of transgenic *MxCS3 A. thaliana* flowers which has five petals accounted for about 45.7% in OE-5 line (44.3% in OE-4), followed by the flowers with four petals and six petals, the ratios were about 23.7 and 18.3%, the flowers with three petals had the smallest proportion, about 14.7%. In contrast, the proportion of the total abnormal petals flowers in WT line was less than 1%.

Discussion

Sequence homologous analysis showed that MxCS3 is a member of the CS family (Fig. 2a), there are only 4.1, 5.2, 12.3, 16.4, 21.5, 21.8, and 23.6% of amino acid differences between MxCS3 and MdCS3, MxCS1, PpCS3, AtCS4, DcCS, NtCS, OsCS, respectively (Fig. 2b). All the CS family includes one conserved CS domain in the C-terminal region (Etienne et al. 2002; Alexandrov et al. 2006; Han et al. 2013a). These results showed that the CS family genes are highly conserved during evolution. Previous reports have indicated that CS genes were widely distributed in apple, peach, *A. thaliana*, carrot, tobacco and rice, and were known to be involved in a variety of processes, including metal transport (Han et al. 2012).

Table 1 Effects of transformation of *MxCS3* on MS agar plates with different Fe concentrations (4, 100 and 400 μM) on fresh weight, root length, content of chlorophyll, CS activity, Fe content, Zn content and citrate acid content of *Arabidopsis*

Parameter	4 μM			100 μM			400 μM		
	WT	OE-4	OE-6	WT	OE-4	OE-6	WT	OE-4	OE-6
Fresh weight (mg *FM*)	195^{B}	494^{A}	489^{A}	453^{A}	461^{A}	459^{A}	109^{C}	298^{B}	323^{B}
Root length (cm)	13.9^{B}	35.4^{A}	29.6^{A}	23.1^{A}	24.2^{A}	23.7^{A}	15.8^{B}	25.1^{A}	27.7^{A}
Chlorophyll content (mg.g^{-1} *FM*)	0.82^{D}	1.88^{C}	1.91^{C}	2.16^{A}	2.27^{A}	2.31^{A}	0.74^{C}	1.59^{B}	1.67^{B}
Citrate synthase activity (U·mg^{-1} *FM*)	892^{B}	4597^{A}	4641^{A}	563^{C}	1248^{B}	1326^{B}	928^{B}	3842^{A}	3937^{A}
Fe content (μg.g^{-1} *DM*)	42^{D}	79^{C}	82^{C}	87^{C}	99^{C}	95^{C}	133^{B}	189^{A}	197^{A}
Zn content (μg.g^{-1} *DM*)	27^{D}	59^{C}	62^{C}	23^{C}	41^{C}	43^{C}	15^{B}	39^{A}	37^{A}
Content of citrate acid (μg·g^{-1} *FM*)	71^{C}	228^{A}	243^{A}	54^{C}	129^{B}	133^{B}	62^{D}	155^{B}	161^{B}

All parameters were measured 14 days after treatments. Each value represents the mean of three experiments with ten replicates in each. Means within a column followed by different letters are significantly different at $P < 0.01$ by SAS

FM fresh mass, *DM* dry mass

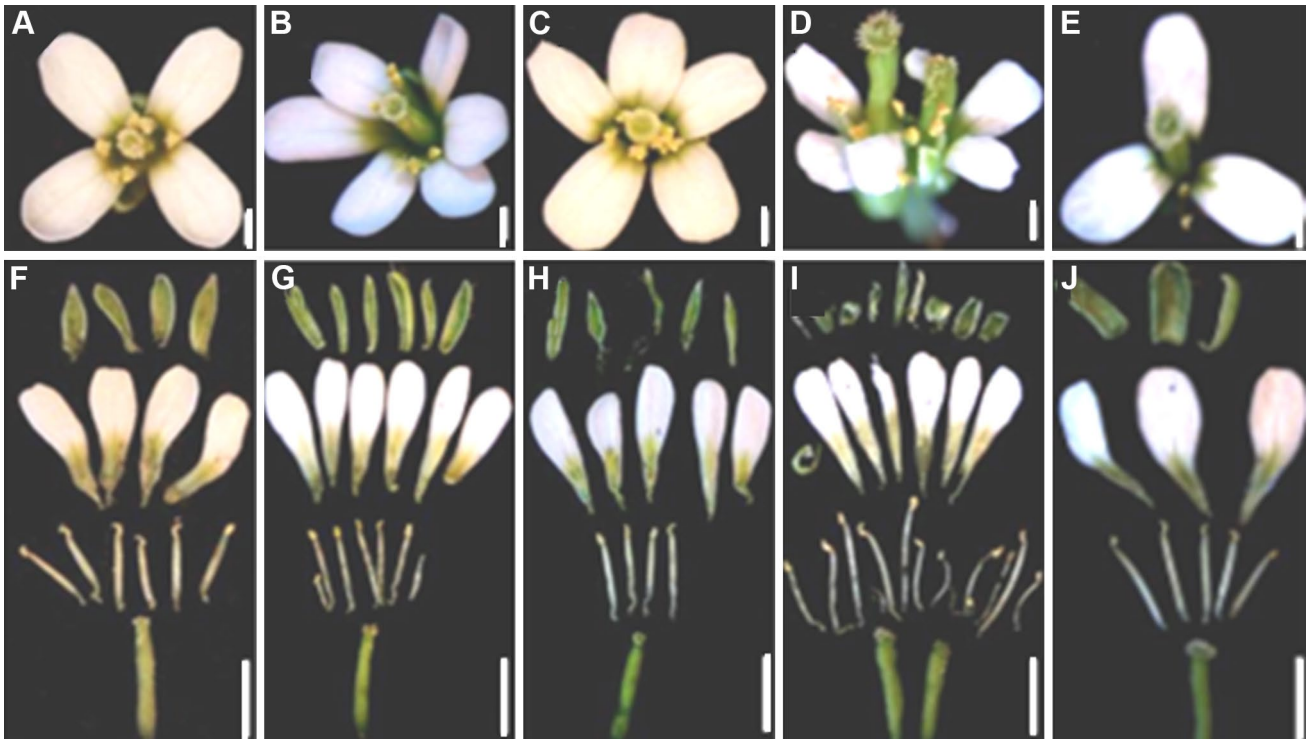

Fig. 6 Flower and flower organ of wild-type *Arabidopsis thaliana* and *MxCS3*-OE transgenic *A. thaliana* (OE-4 and OE-5). **a** Wild-type *Arabidopsis* flower; **b–e** *MxCS3*-OE *Arabidopsis* flowers; **f** All organs (calyxes, petals, stamens and pistil) of WT *Arabidopsis* flower (**a**); **g–j** All organs (calyxes, petals, stamens and pistils) of *MxCS3*-OE *Arabidopsis* flowers (**b–e**). *Scale bars* 0.6 mm in (**a–e**) and 3 mm in (**f–j**)

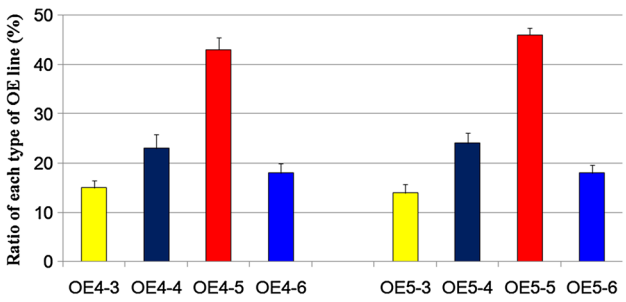

Fig. 7 Proportions of each type flower with different number of petals of *MxCS3*-OE transgenic *Arabidopsis thaliana*. OE4-3, OE4-4, OE4-5, OE4-6, OE5-3, OE5-4, OE5-5, OE5-6 are represented different transgenic *Arabidopsis* lines (OE4 and OE5) with different number of petals (3, 4, 5 and 6), respectively

Subcellular localization has revealed that the MxCS3 is a mitochondrion and cytoplasmic membrane localization protein (Fig. 3), which is consistent with MxCS2 (Han et al. 2015a) and another CS protein into mitochondrion (Alexandrov et al. 2006). Previous studies showed that the expected location of citrate synthases in *A. thaliana* were mitochondria, peroxisome or glyoxysome and had a conservative 'RLAVL' box in the N-terminus (Slabas et al. 2004). The citrate synthases in oilseed plants, such as soybean, sunflower, and canola were located in peroxisome (Eckardt 2005). Presumably, the protein may have an uncertain or unknown area which affects the results of subcellular localization, leading to the localization in mitochondrion and cytoplasmic membrane.

The expression of *MxCS3* was much enriched in new leaf and root than that in phloem and mature leaf, but very low in the xylem (Fig. 4a). This expression pattern indicated that *MxCS3* may play an important role in active organs, which was in accord with the expression level of *MxCS1* and *MxCS2* gene in different parts in *M. xiaojinensis* in normal Fe concentration (Han et al. 2012, 2015a). When treated with IAA and ABA, high and low Fe stresses, the expression of *MxCS3* in leaf, phloem and root was markedly affected. It is possible that *MxCS3* plays a key role in regulating Fe stress response in *M. xiaojinensis*. IAA and ABA are considered as signals of Fe stress in plants (Schikora and Schmidt 2001; Schmidt et al. 2000), and IAA treatment affected the expression of *MxCS3*.

The results showed that the expression level of *MxCS3* increased in new leaf (Fig. 4b), phloem (Fig. 4d) and root (Fig. 4e) under low Fe treatment after 2, 4, 8 h, respectively, while decreased slightly after 12 h. It is possible that

when exposed to low Fe stress, *M. xiaojinensis* increased the expression of *MxCS3* to accelerate the synthesis of CS and CA. Consequently, higher concentration of CA in plants promoted the uptake of Fe from poor Fe environment (Gray et al. 1996). A possible explanation for the lower expression of *MxCS3* under 12 h treatment is that there has been enough CA accumulation for the Fe absorption at this point. Conversely, the expression of *MxCS3* in these parts was down-regulated in high Fe environment to reduce the synthesis of CS and CA so that the uptake of Fe from the environment decreased. The expression level of *MxCS3* in mature leaf (Fig. 4c) was just opposite to the above parts under Fe stress concentration, which decreased when dealt with low Fe treatment but increased when dealt with high Fe stress. In low Fe environment, Fe was preferentially provided to active parts such as new leaf, phloem and root, so the expression level of *MxCS3* in these parts increased, but decreased in mature leaf. The expression level increased in mature leaf when dealt with high Fe stress for removing Fe toxicity. The expression levels of *MxCS1* and *MxCS2* increased in active organs, such as root and new leaf when dealt with low Fe stress but decreased when dealt with high Fe treatment (Han et al. 2012, 2015a).

The FRD mutants (such as *Atfrd3* and *Osfrdl1*) have also been studied, and the results showed that the mutants lack a protein responsible for efflux of citrate in cells of the xylem vasculature (Durrett et al. 2007; Yokosho et al. 2009) as well as in inter-cellular spaces lacking symplastic connections (Roschzttardtz et al. 2011). The above studies demonstrated that FRD mediated-Cit efflux is required to sustain normal rates of Fe transport. The expression levels of *MxCS1* and *MxCS2* were strongly affected by Fe stress in *M. xiaojinensis* seedlings, in new leaf and mature leaf, which were just opposite (Han et al. 2013a, 2015a). The effects of high and low Fe stresses on expression levels of *MxCS3* in new leaf, mature leaf, root, and phloem were obvious in this study, except in xylem (not presented here). It is possible the xylem is not an active organ and is constituted almost by dead cells. Low Fe stress induced the increases of the expressions of three *M. xiaojinensis* citrate synthase genes *MxCS1, MxCS2* and *MxCS3* play a role in the synthesis of CS and citric acid. Thus, the CS and CA in *M. xiaojinensis* are higher under low Fe stress (Wu et al. 2012). These results are consistent with previous findings that higher concentration of CA in plants promoted the uptake of Fe from poor Fe environment (Gray et al. 1996; Rellán-Álvarez et al. 2010).

The expression levels of *MxCS1* and *MxCS2* in root and mature leaf of *M. xiaojinensis* were strongly affected by IAA treatment, but weakly by ABA treatment (Han et al. 2013a, 2015a). However, the expression levels of *MxCS3* in new leaf, mature leaf, phloem, and root of *M. xiaojinensis* were markedly affected by IAA and ABA treatments. Fe-deficiency also induced IAA level increase in the shoot apex of *M. xiaojinensis* and treatments of IAA to the shoot apex triggered Fe deficiency responses (Wu et al. 2012). Based on the previous studies and theories, we reckon that IAA and ABA treatments induce Fe deficiency responses, such as the increased expression of *MxCS3* in the above parts and the *MxCS3* gene probably has affected Fe transport.

Ectopic expression of *MxCS3* enhanced the tolerance to Fe stress at both high and low concentrations in transgenic *A. thaliana*. It is possible that *MxCS3* plays a crucial role in helping plants to survive from Fe stress by regulating the synthesis of citric acid. Higher content of CA in *MxCS3*-OE *A. thaliana* helped to extract Fe from poor Fe environment (Wang et al. 2013; Han et al. 2013a, 2015a). Meanwhile, high concentration of citric acid was also helpful in chelating redundant metal ions for detoxification when plants were exposed to high metal environment. Citrate is involved in the detoxification of Al via complexation either externally [Al-induced root-secretion of organic acids (Ma 2007)] or internally [occurrence of Al-citrate complex in xylem sap (Ma and Hiradate 2000)]. Therefore, this theory explained why transgenic *A. thaliana* showed higher tolerance to high Fe stress. Moreover, the higher Fe level induced by high concentration of CA leads to the higher content of chlorophyll in *MxCS3*-OE lines, since Fe is a necessary component of chloroplast. Ectopic expression of *MxCS1* and *MxCS2* also improved Fe stress tolerance in transgenic *Arabidopsis* (Han et al. 2012, 2015a). The results of this study showed that ectopic expression of *MxCS3* improved the tolerance to Fe stress in transgenic *A. thaliana* (Fig. 5), but also led to increased fresh weight, root length, CS activity, and contents of chlorophyll, citrate acid, Fe and Zn, especially when dealt with Fe stress (Table 1).

More importantly, it is the first time we found that ectopic expression of *MxCS3* resulted in abnormal flowers in transgenic *A. thaliana* (Fig. 6), including abnormal shape and the number of flower organs. The proportion of transgenic *MxCS3 A. thaliana* flowers with normal number of petal is less than 25% (Fig. 7) while the proportion in WT line is more than 99%. Previous study found that increased expression of *MxCS1* in transgenic tobacco resulted in early-flowering and morphological abnormalities flowers (Han et al. 2013a). Metal ions (particularly Zn and Fe) participate in normal flower development (Conte and Walker 2011). Metal ions are also very important for reproductive development of plants, because they are components of many critical proteins during this stage (Kim and Guerinot 2007). The higher contents of metal ions (especially Zn and Fe) in transgenic *Arabidopsis* under Fe stress (Table 1) probably affect the activity of critical proteins in flower development, and the function of transcriptional regulatory

proteins, such as Zn finger, and RING finger domains. Zn plays an essential role in some structural motifs of transcriptional regulatory proteins, including Zn finger, Zn cluster, and RING finger domains (Kapoor et al. 2002). The increased contents of metal ions in transgenic *Arabidopsis* were due to the elevated concentration of CA. CA, acting as a metal carrier, can help to transfer metal ions to organs such as leaves. CA could also be involved in regulating functions of metal-requiring proteins (such as Zn finger proteins), thus it may affect the number of flower organs, determine the shape of flower organs. Hence, the abnormally shaped flowers of transgenic *A. thaliana* were produced as a result.

Previously, we have not found that the *MxCS1*-OE or *MxCS2*-OE transgenic *A. thaliana* flowers appear to be misshappened, one possible reason is that the flower of *A. thaliana* is so small or the functions of *MxCS1* and *MxCS2* were not strong enough. Compared with *MxCS1* (Han et al. 2012, 2013a) and *MxCS2* (Han et al. 2015a), the expressions of *MxCS3* in young and mature leaf of *M. xiaojinensis* changed more quickly with higher amplitude when dealt with Fe stress. The contents of CA and Fe in *MxCS3*-OE transgenic *A. thaliana* are higher than *MxCS1*-OE and *MxCS2*-OE lines. Hence, the *MxCS3* gene is more likely the key gene of *MxCS* gene family than *MxCS1* and *MxCS2*.

These results suggested that *MxCS3* might be one of the upstream regulator genes of Fe stress, and the ectopic expression of *MxCS3* can enhance the Fe stress tolerance in *A. thaliana*. The role of *MxCS3* in inducing misshapen flowers indicates its great potential application in the breeding of horticultural plants especially ornamental flowers. Clarifying the role of the different domains of *MxCS3* in stress response will be helpful in breeding stress-resistant *Malus* by gene transfer. Further experiments are required to identify other functions of *MxCS3* gene.

Acknowledgements This project was supported by National Natural Science Foundation of China (31301757), Natural Science Foundation of Heilongjiang Province of China (C2015015), Academic Backbone Project of Northeast Agricultural University (15XG06), Scientific Research Fund of Heilongjiang Provincial Education Department (12541004), Heilongjiang Postdoctoral Science Foundation (LBH-Q16020), the Open Project of Key Laboratory of Biology and Genetic Improvement of Horticultural Crops (Northeast Region), Ministry of Agriculture (neauhc201602) and the Science and Technology Innovation Project for Undergraduate of Biology and Genetic Improvement of Horticultural Crops (Northeast Region), Ministry of Agriculture (NEAU-HC-UNDS-201606). The authors are grateful Dr. Wei Liu for the English correction of the paper.

References

Abadía J, López-Millán AF, Rombolà A, Abadía A (2002) Organic acids and Fe deficiency: a review. Plant Soil 241:75–86

Alexandrov NN, Troukhan ME, Brover VV, Tatarinova T, Flavell RB, Feldmann KA (2006) Features of *Arabidopsis* genes and genome discovered using full-length cDNAs. Plant Mol Biol 60(1):69–85

An G, Watson BD, Chang CC (1988) Transformation of tobacco, tomato, potato, and *Arabidopsis* using a binary Ti vector system. Plant Physiol 81:301–305

Aono M, Kubo A, Saji H, Tanaka K, Kondo N (1993) Enhanced tolerance to photo-oxidative stress of transgenic *Nicotiana tabacum* with high chloroplastic glutathione reductase activity. Plant cell Physiol 34:129–136

Cataldo DA, McFadden KM, Garland TR, Wildung RE (1988) Organic constituents and complexation of nickel(II), iron(III), cadmium(II) and plutonium(IV) in soybean xylem exudates. Plant Physiol 86:34–39

Conte SS, Walker EL (2011) Transporters contributing to iron trafficking in plants. Mol Plant 4:464–476

Durrett TP, Gassmann W, Rogers EE (2007) The FRD3-mediared efflux of citrate into the root vasculature is necessary for efficient iron translocation. Plant Physiol 144:197–205

Eckardt NA (2005) Peroxisomal citrate synthase provides exit route from fatty acid metabolism in oilseeds. Plant Cell 17(7):1863–1865

Etienne C, Moing A, Dirlewanger E, Raymond P, Monet R, Rothan C (2002) Isolation and characterization of six peach cDNAs encoding key proteins in organic acid metabolism and solute accumulation: involvement in regulating peach fruit acidity. Plant Physiol 114:259–270

Gray NK, Pantopoulos K, Danderkar T, Ackrell BA, Hentze MW (1996) Translational regulation of mammalian and drosophila citric acid cycle enzymes via iron-responsive elements. Proc Natl Acad Sci USA 93:4925–4930

Guerinot ML, Yi Y (1994) Iron: nutritious, noxious and not readily available. Plant Physiol 104:815–820

Han ZH, Shen T, Korcak RF, Baligar VC (1998) Iron absorption by iron-efficient and inefficient species of apples. J Plant Nutr 2:181–190

Han DG, Wang Y, Zhang L, Ma L, Zhang XZ, Xu XF, Han ZH (2012) Isolation and functional characterization of *MxCS1*: a gene encoding a citrate synthase in *Malus xiaojinensis*. Biol Plant 56(1):50–56

Han DG, Wang L, Wang Y, Yang GH, Gao C, Yu ZY, Li TY, Zhang XZ, Ma L, Xu XF, Han ZH (2013a) Overexpression of *Malus xiaojinensis CS1* gene in tobacco affects plant development and increases iron stress tolerance. Sci Hortic 150:65–72

Han DG, Yang GH, Xu KD, Shao Q, Yu ZY, Wang B, Ge QL, Yu Y (2013b) Overexpression of a *Malus xiaojinensis Nas1* gene influences flower development and tolerance to iron stress in transgenic tobacco. Plant Mol Biol Rep 31:802–809

Han DG, Shi Y, Wang B, Liu W, Yu ZY, Lv BY, Yang GH (2015a) Isolation and preliminary functional analysis of *MxCS2*: a gene encoding a citrate synthase in *Malus xiaojinensis*. Plant Mol Biol Report 33:133–142

Han DG, Shi Y, Yu ZY, Liu W, Lv BY, Wang B, Yang GH (2015b) Isolation and functional analysis of *MdCS1*: a gene encoding a citrate synthase in *Malus domestica* (L.) Borkh. Plant Growth Regul 75:209–218

Hell R, Stephan UW (2003) Iron uptake, trafficking and homeoststasis in plants. Planta 216:541–551

Jelali N, Dell'orto M, Abdelly C, Gharsalli M, Zocchi G (2010) Changes of metabolic responses to direct and induced Fe deficiency of two *Pisum sativum* cultivars. Environ Exp Bot 68(3):238–246

Jiang KY, Zhou MB (2016) Cloning and functional characterization of *PjPORB*, a member of the *POR* gene family in *Pseudosasa japonica* cv. Akebonosuji. Plant Growth Regul 79:95–106

Kapoor S, Kobayashi A, Takatsuji H (2002) Silencing of the tapetum-specific zinc finger gene TAZ1 causes premature degeneration of tapetum and pollen abortion in petunia. Plant Cell 14:2353–2367

Kim SA, Guerinot ML (2007) Mining iron: iron uptake and transport in plants. FEBS Lett 581:2273–2280

Leek BT, Mudaliar SR, Henry R, Mathieu-Costello O, Richardson RS (2001) Effect of acute exercise on citrate synthase activity in untrained and trained human skeletal muscle. Am J Physiol Regul Integr Comp Physiol 280(2):441–447

Li P, Qi JL, Wang L, Huang QN, Han ZH, Yin LP (2006) Functional expression of *MxIRT1*, from *Malus xiaojinensis* complements an iron uptake-deficient yeast mutant for plasma membrane targeting via a membrane vesicles trafficking process. Plant Sci 171:52–59

Ling HQ, Koch G, Baumlein H, Ganal MW (1999) Map-based cloning of chloronerva, a gene involved in iron uptake of higher plants encoding nicotianamine synthase. Proc Natl Acad Sci USA 96:7098–7103

Livak KJ, Schmittgen TD (2001) Analysis of relative gene expression data using real-time quantitative PCR and the $2^{-\Delta\Delta CT}$ method. Methods 25:402–408

López-Millán AF, Morales F, Abadía A, Abadía J (2001) Iron deficiency-associated changes in the composition of the leaf apoplastic fluid from field-grown pear (*Pyrus communis* L.) trees. J Exp Bot 52:1489–1498

López-Millán AF, Morales F, Gogorcena Y, Abadía A, Abadía J (2009) Metabolic responses in iron deficient tomato plants. J Plant Physiol 166:375–384

López-Millán AF, Grusak MA, Abadía J (2012) Carboxylate metabolism changes induced by Fe deficiency in barley, a Strategy II plant species. J Plant Physiol 169(11):1121–1124

Ma JF (2007) Syndrome of aluminum toxicity and diversity of aluminum resistance in higher plants. Int Rev Cytol 264:225–252

Ma JF, Hiradate S (2000) Form of aluminium for uptake and translocation in buckwheat (*Fagopyrum esculentum Moench*). Planta 211(3):355–360

Marschner H (2012) Marschner's mineral nutrition of higher plants [M]. Academic Press, London

Marschner H, Romheld V (1994) Strategies of plants for acquisition of iron. Plant Soil 165:261–274

Martínez-Cuenca MR, Iglesias DJ, Talón M, Abadía J, López-Millán AF, Primo-Millo E, Legaz F (2013) Metabolic responses to iron deficiency in roots of Carrizo citrange [*Citrus sinensis* (L.) Osbeck. × *Poncirus trifoliata* (L.) Raf.]. Tree Physiol 33(3):320–329

Rellán-Álvarez R, Giner-Martínez-Sierra J, Orduna J, Orera I, Rodríguez-Castrillón JA, García-Alonso JI, Abadía J, Álvarez-Fernández A (2010) Identification of a tri-iron(III), tri-citrate complex in the xylem sap of iron-deficient tomato resupplied with iron: new insights into plant iron long-distance transport. Plant Cell Physiol 51(1):91–102

Rombolà AD, Brüggemann W, López-Millán AF, Tagliavini M, Abadía J, Marangoni B, Moog PR (2002) Biochemical responses to iron deficiency in kiwifruit (*Actinidia deliciosa*). Tree Physiol 22(12):869–875

Romheld V, Marschner H (1986) Evidence for a specific system for iron phytosiderophores in roots of grasses. Plant Physiol 80:175–180

Roschzttardtz H, Séguéla-Arnaud M, Briat JF, Vert G, Curie C (2011) The FRD3 citrate effluxer promotes iron nutrition between symplastically disconnected tissues throughout *Arabidopsis* development. Plant Cell 23(7):2725–2737

Schikora A, Schmidt W (2001) Acclimative changes in root epidermal cell fate in response to Fe and P deficiency: a specific role for auxin? Protoplasma 218:67–75

Schmidt W, Tittel J, Schikora A (2000) Role of hormones in the induction of iron deficiency responses in *Arabidopsis* roots. Plant Physiol 122(4):1109–1118

Shen J, Xu XF, Li TZ, Cao DM, Han ZH (2008) An MYB transcription factor from *Malus xiaojinensis* has a potential role in iron nutrition. J Integr Plant Biol 50(10):1300–1306

Slabas AR, Ndimba B, Simon WJ, Chivasa S (2004) Proteomic analysis of the *Arabidopsis* cell wall reveals unexpected proteins with new cellular locations. Biochem Soc Trans 32(3):524–528

Takahashi M, Terada Y, Nakai I, Nakanishi H, Yoshimura E, Mori S, Nishizawa NK (2003) Role of nicotianamine in the intracellular delivery of metals and plant reproductive development. Plant Cell 15:1263–1280

Takita E, Koyama H, Shirano Y, Shibata D, Hara T (1999) Structure and expression of the mitochondrial citrate synthase gene in carrot cells utilizing Al-phosphate. Soil Sci Plant Nutr 45:197–205

Thimm O, Essigmann B, Kloska S, Altmann T, Buckhout TJ (2001) Response of *Arabidopsis* to iron deficiency stress as revealed by microarray analysis. Plant Physiol 127(3):1030–1043

Wang YP, Wu YH, Zheng GH, Zhang JP, Xu GD (2013) Effects of potassium on organic acid metabolism of Fe-sensitive and Fe-resistant rices ('*Oryza sativa*' L.). Aust J Crop Sci 7(6):843

Wu T, Zhang HT, Wang Y, Jia WS, Xu XF, Zhang XZ, Han ZH (2012) Induction of root Fe(lll) reductase activity and proton extrusion by iron deficiency is mediated by auxin-based systemic signalling in *Malus xiaojinensis*. J Exp Bot 63:859–870

Xu HM, Wang Y, Chen F, Zhang XZ, Han ZH (2011) Isolation and characterization of the iron-regulated *MxbHLH01* gene in *Malus xiaojinensis*. Plant Mol Biol Rep 29:936–942

Yang GH, Li J, Liu W, Yu ZY, Shi Y, Lv BY, Wang B, Han DG (2015) Molecular cloning and characterization of *MxNAS2*, a gene encoding nicotianamine synthase in *Malus xiaojinensis*, with functions in tolerance to iron stress and misshapen flower in transgenic tobacco. Sci Hortic 183:77–86

Yin LL, Wang Y, Yan MD, Zhang XZ, Pan HF, Xu XF, Han ZH (2013) Molecular cloning, polyclonal antibody preparation, and characterization of a functional iron-related transcription factor IRO2 from *Malus xiaojinensis*. Plant Physiol Biochem 67:63–70

Yokosho K, Yamaji N, Ueno D, Mitani N, Ma JF (2009) OsFRDL1 is a citrate transporter required for efficient translocation of iron in rice. Plant Physiol 149(1):297–305

Zhang YG, Kong J, Wang Y, Xu XF, Liu LL, Li TZ, Han ZH, Zhu YJ (2009) Isolation and characterisation of a nicotianamine synthase gene *MxNas1* in *Malus xiaojinensis*. J Hortic Sci. Biotechnol 84(1):47–52

Zhang Q, Wang Y, Zhang XZ, Yin LL, Wu T, Xu XF, Jia WS, Han ZH (2012) Cloning and characterization of *MxVHA-c*, a vacuolar H^+-ATPase subunit C gene related to Fe efficiency from *Malus xiaojinensis*. Plant Mol Biol Rep 30:1149–1157

Zhu YJ, Wang Y, Kong J, Wang J, Zhang XZ, Han ZH (2009) Role of *SAMS* gene in Fe uptake mechanism of *Malus xiaojinensis*. Acta Hortic 2:463–469